Annealing of Co-Cr dental alloy: effects on nanostructure and Rockwell hardness

Simel Ayyıldız[1*], DDS, PhD, Elif Hilal Soylu[2], DS, PhD, Semra İde[3], DS, PhD, Selim Kılıç[4], MD, Cumhur Sipahi[1], DDS, PhD, Bulent Pişkin[1], DDS, PhD, Hasan Suat Gökçe[5], DDS, PhD

[1]Department of Prosthodontics, Dental Health Sciences Center, Gulhane Military Medical Academy, Ankara, Turkey
[2]Department of Physics, Karadeniz Technical University, Faculty of Science and Literature, Trabzon, Turkey
[3]Department of Physics Engineering, Faculty of Engineering, Hacettepe University, Ankara, Turkey
[4]Department of Public Health, Gulhane Military Medical Academy, Ankara, Turkey
[5]Dental Health Service, Beytepe Military Hospital, Ankara, Turkey

PURPOSE. The aim of the study was to evaluate the effect of annealing on the nanostructure and hardness of Co-Cr metal ceramic samples that were fabricated with a direct metal laser sintering (DMLS) technique. **MATERIALS AND METHODS.** Five groups of Co-Cr dental alloy samples were manufactured in a rectangular form measuring 4 × 2 × 2 mm. Samples fabricated by a conventional casting technique (Group I) and prefabricated milling blanks (Group II) were examined as conventional technique groups. The DMLS samples were randomly divided into three groups as not annealed (Group III), annealed in argon atmosphere (Group IV), or annealed in oxygen atmosphere (Group V). The nanostructure was examined with the small-angle X-ray scattering method. The Rockwell hardness test was used to measure the hardness changes in each group, and the means and standard deviations were statistically analyzed by one-way ANOVA for comparison of continuous variables and Tukey's HSD test was used for post hoc analysis. *P* values of <.05 were accepted as statistically significant. **RESULTS.** The general nanostructures of the samples were composed of small spherical entities stacked atop one another in dendritic form. All groups also displayed different hardness values depending on the manufacturing technique. The annealing procedure and environment directly affected both the nanostructure and hardness of the Co-Cr alloy. Group III exhibited a non-homogeneous structure and increased hardness (48.16 ± 3.02 HRC) because the annealing process was incomplete and the inner stress was not relieved. Annealing in argon atmosphere of Group IV not only relieved the inner stresses but also decreased the hardness (27.40 ± 3.98 HRC). The results of fitting function presented that Group IV was the most homogeneous product as the minimum bilayer thickness was measured (7.11 Å). **CONCLUSION.** After the manufacturing with DMLS technique, annealing in argon atmosphere is an essential process for Co-Cr metal ceramic substructures. The dentists should be familiar with the materials that are used in clinic for prosthodontics treatments. ***[J Adv Prosthodont 2013;5:471-8]***

KEY WORDS: Dental alloys; Hardness test; X-ray microanalysis; Metal ceramic alloys

Corresponding author:
Simel Ayyıldız
Gulhane Military Medical Academy, Dental Health Sciences Center
Department of Prosthodontics, 06018, Etlik, Ankara, Turkey
Tel. 903123046058: e-mail, simelayyildiz@gmail.com
Received June 20, 2013 / Last Revision November 6, 2013 / Accepted November 17, 2013

INTRODUCTION

Dental alloys have been used in dentistry for prosthetic rehabilitation for hundred years.[1] Precious or alternative alloys are still in use for metallic structures of fixed dental prosthesis. However, the use of precious alloys is limited because of their high costs, and for this reason, non-precious dental alloys have been introduced to the dental field.[2] Currently, the most used non-precious metallic alloys are cobalt-chromium (Co-Cr) and nickel-chromium (Ni-Cr), as their hardness, elasticity modulus, and tensile strength are suitable for metal ceramic restorations.[3] However, the

European Union and ADA have proposed to retire alloys containing nickel because of the possible allergic interaction of nickel with humans.[4] Therefore, recently, the widespread use of Co-Cr alloys has been seen in the dental field.

Conventional casting method is the most frequently used technique for manufacturing Co-Cr alloy fixed dental prostheses. In recent years, modern computer-aided technologies for manufacturing individual prostheses have been gaining popularity in the field of dental technology.[5] Computer-aided design (CAD) and computer-aided manufacturing (CAM) technologies are used frequently in the dental field to fabricate prostheses ranging from crowns to long-span fixed dental prosthesis and from removable prostheses to dental implants.[6] The term CAD/CAM implies that the system can be used both for designing a product and for controlling the manufacturing process.[7] The actual fabrication of a Co-Cr product is carried out by computer numerical control (CNC) milling machines or direct metal laser sintering (DMLS) machines.[8,9] These systems were developed to address a number of disadvantages of the traditional casting method like human induced errors, production cost and dimensional stability.[10,11]

The microstructure of metal alloys is strongly influenced by the manufacturing process.[12] Moreover, the quality of a material and thus the clinical chances of success are directly affected by controlling the manufacturing environment.[13-15] New manufacturing processes such as metal injection molding and powder-metallurgical techniques are being developed to achieve dental alloys with better microstructure and mechanical properties.[10,16] With the industrial production of Co-Cr in the form of blanks, increasingly homogeneous metal structures can be obtained. These blanks have been used in CNC milling machines for manufacturing crowns, long-span fixed dental prosthesis and other prosthetic devices.[2] In dentistry, manufacturing techniques such as casting and CNC milling methods are well known to dentists and dental technicians. Only recently, the DMLS technique has started gaining attention in this field. However, the manufacturing stages of this technique and factors that affect product quality are not well known.

Sintering is a method used to create objects from powders. The effects of sintering are based on atomic diffusion, which occurs much faster at higher temperatures.[17] During sintering, the atoms in powder particles diffuse across particle boundaries; this fuses the particles together to create a single solid piece.[18] DMLS is an additive metal fabrication technology that involves the use of a high-powered Ytterbium (Yb)-fiber optic laser.[19] In this technology, metal powder is melted locally with a focused laser beam and fused into a solid part. The parts are built up additively, layer by layer, each of which is 10-30 μm thick.[20] When compared to casting technique, DMLS technology affords highly accurate production of materials with higher surface quality and increased mechanical properties.[11,21]

When metal alloys are manufactured with sintering techniques, a heat treatment process called "annealing" is used to advance the material toward its equilibrium state.[22] The procedure for annealing an object involves heating it above the critical temperature, maintaining it at a stable temperature, and then cooling it down.[23,24] The most important aims of annealing are to increase ductility of an object, accelerate relief of internal stresses, soften material, and refine the structure by making it homogeneous.[9,22,23] After manufacturing Co-Cr prosthetic sub structures by using the DMLS technique, annealing is required to obtain homogeneous metallic structures.[9,20] However, changes in temperature, atmosphere, or both of them during the annealing process affect the microstructure and hardness of the alloy.[24]

Many techniques are available for evaluating the structural characteristics of metal alloys. Small angle X-ray scattering (SAXS) is one such technique used for the structural characterization of solid and fluid materials in the nanometer (nm) range. Measurements are commonly performed in transmission geometry by using a narrow, well-collimated, and intense X-ray beam. Some typical applications comprise the determination of nanoparticle and pore size distributions of specific surface areas and the structural analysis in inhomogeneous particles. Further, the technique may yield information about the aggregation behavior of nanoparticles.[25] Detailed information about the nanostructure of metallic materials, such as the analyses of fractal dimensions, distance distribution function, and fitting function, may be obtained by using data from SAXS analysis. In the analysis of fractal dimension, the mass fractals are examined and information about the structural formation of the solid object is obtained. The analysis of the distance distribution function yields the distribution of particle dimensions or of the inter-particle distances. The obtained data indicate the structural homogeneity of the object.[26] SAXS profiles for nanosized surface aggregates can be modeled by an intensity equation defined by the addition of scattering intensity functions related to cylindrical and lamellar aggregations [$I(q) = I_1(q) + I_2(q)$] with a software program (IGOR Pro 1998-2008 WaveMetrics). The cylindrical and lamellar functions are used in the fitting procedure; thus, detailed information about the length of the cylinders and the thickness of the layers in the structural formation of the object may be obtained.[25,26]

The aim of this study was to compare the nanostructures and hardness of Co-Cr dental alloys manufactured with different techniques and to find the effect of annealing conditions to the alloys that was produced with DMLS method.

MATERIALS AND METHODS

Five groups of Co-Cr dental alloy samples were manufactured in a rectangular form measuring 4 mm × 2 mm × 2 mm. In Group I, conventional Co-Cr (Remanium® 2000+, Dentaurum, Pforzheim, Germany) samples were manufactured by the lost wax technique in an induction-casting machine (Fornax GEU, Bego, Bremen, Germany). After modeling with green inlay casting wax (n=15) (Bego, Bremen, Germany), specimens were sprued and invested in

phosphate-bonded investment (Bellavest SH, Bego, Bremen, Germany). After the final setting of the investment, each ring was put into a furnace (Miditherm MP, Bego, Bremen, Germany) to evaporate the wax material. Casting was accomplished according to the manufacturer's instructions. After cooling at room temperature, the samples were cleaned and sandblasted by airborne abrasion with 250 μm Al_2O_3 particles. The samples in Group II were obtained from the center of a prefabricated Co-Cr milling blank (Remanium® star milling blank, Dentaurum, Pforzheim, Germany) manually by using a diamond bur under water-cooling (n=15). The surfaces of the samples were finished with 400 grit sandpaper (CarbiMet 2 Paper Discs, Buehler, Lake Bluff, IL, USA) and sandblasted by airborne abrasion with 250 μm Al_2O_3 particles.

The samples in Groups III, IV, and V were manufactured with a DMLS machine (M2 Cusing, ConceptLaser GmBH, Lichtenfels, Germany) after 3D CAD (n=15 for each group). For laser-aided production of samples, Co-Cr nanopowder (Remanium® star CL, Dentaurum, Pforzheim, Germany) was used. After production, the samples were randomly divided into 3 groups (Groups III, IV, and V). In Group III, the samples were only sandblasted by airborne abrasion with 250 μm Al_2O_3 particles after manufacturing. In Group IV, the samples were annealed in argon atmosphere (XD 1600A, Zhengzhou Brother Furnace, Co., Ltd, Henan, China) under controlled temperature according to the manufacturer's instructions. During annealing, the samples were heated to 1150℃ over the course of 173 minutes, stabilized at this temperature for 232 minutes, cooled to 300℃ in 593 minutes, removed from the furnace, and left to cool at room temperature. In Group V, the samples were annealed in atmospheric oxygen condition (XD 1600A, Zhengzhou Brother Furnace, Co., Ltd, Henan, Chinaunder) the same controlled annealing process with Group IV. In both Groups IV and V, all samples were sandblasted by airborne abrasion with 250 μm Al_2O_3 particles after annealing.

The nanostructure was examined with the SAXS method by using a HECUS-SAXS system3 (Hecus X-ray systems, Brucker Austria GmbH, Graz, Austria) with CuKα (λ = 1.54 Å) radiation operated at 50 kV and 50 mA, line collimation, and position sensitive detectors (~54 μm resolution, 1024 channels). SAXS measurements were performed at room temperature in a 600 second time interval. Analyses of fractal dimension, distance distribution function, and fitting function were performed according to the SAXS measurements. In analyses of fractal dimension, logarithmic plots were prepared for the samples and fitted to Equation 1 to analyze the fractal structure with spherical fractal units. Equation 1 is well known scattering intensity function for densed/fractal nanostructured systems[25] and can be written as follows:

$$I(q) = P(q).S(q) + bkgd$$
$$P(q) = \text{ø}.V_p.\Delta\rho^2.F(qR_0^2)^2$$
$$V_p = 4/3.\pi.R_0^3$$
$$F(x) = \frac{3[\sin(x) - x\cos(x)]}{x^3}$$
$$S(q) = 1 + \frac{\sin[(D_f - 1)\tan^{-1}(q\xi)].D_f\Gamma(D_f - 1)}{(qR_0)^{D_f}[1 + 1/(q^2\xi^2)]^{(D_f - 1)/2}}$$

In the formulation P(q) is including information about; number of particles per unit volume (ø), volume of particle (V_p), electron density (Δρ) and form factor ($[F(qR_g^2)]^2$), F(x) is the globular form of the nanoaggregations and S(q) is the structure function accounting for short range spatial correlated particles. Also, bkgd (or bkg) in the formulation indicates the background scattering density, R_g, ξ, and D_f are size of fractal unit, cluster and maximum sizes of fractal regions, respectively. These structural parameters were also calculated according to the fitted curves of SAXS analyses.

In analyses of distance distribution function, the effective radius of the particles (Rg) and maximum effective size of the nanoparticles (maximum extent) were also calculated according to the fitted curves of SAXS analyses.

The fitting function was used for calculating the radius and length of the cylinders and also the bilayer thickness of the lamellas. Thus, the SAXS data of the samples fit the sum of the cylindrical and lamellar functions. The cylindrical function used in the fitting procedure is expressed as follows.

$$I(q) = \text{ø}P_1(q) + bkg$$

The form factor of cylindrical particles, $P_1(q)$, is given as follows.

$$P_1(q) = \frac{scale}{V_{cyl}}\int_0^{\pi/2} f^2(q,\alpha)\sin\alpha d\alpha$$

$$f(q,\alpha) = 2(\rho_{cyl} - \rho_{solv})V_{cyl}\, j_0(qH\cos\alpha)\frac{J_1(qr\sin\alpha)}{(qr\sin\alpha)}$$

$$V_{cyl} = \pi r^2 L$$
$$j_0(x) = \sin(x)/x$$

Here, q is the scattering vector; α is the angle between the cylinder axis and the scattering vector; and L, H, r, and V are the length, semi-length, radius, and volume, respectively, of the cylinder. In addition, ø is the particle volume fraction, ρ_{cyl} is the scattering length density for the cylinder, ρ_{solv} is the scattering length density for the solvent, and $J_1(x)$ is the Bessel function.

The lamellar function used in the fitting procedure is defined below as

$$I_2(q) = scale\frac{2\pi P_2(q)}{\delta q^2} + bkg$$

Here, $P_2(q)$, the form factor of lamellar particles, is given by

$$P_2(q) = \frac{2\Delta\rho^2}{q^2}[1 - \cos(q\delta)e]^{-q^2\sigma^2/2}$$
$$\Delta\rho = \rho_{bil} - \rho_{solv}$$

Here, δ is the bilayer thickness, σ is the polydispersity (alteration in bilayer thickness), q is the scattering vector, $\Delta\rho$ is the scattering contrast, and ρ_{bil} and ρ_{solv} are the scatter-

ing length densities for the bilayer and solvent, respectively.

The Rockwell hardness (HRC) was measured under 150 kgf/50 s (Time TH3000, Geneq Inc., Montréal, Canada) with a 120° diamond cone and recorded digitally. SPSS software program (SPSS 15.0, SPSS Inc., Chicago, IL, USA) was used to statistically analyze hardness measurements. Descriptive statistics were presented as mean ± standard deviation. One-way analysis of variance (ANOVA) was used for comparisons of continuous variables. Tukey's honestly significant difference (HSD) test was used for post hoc analysis. A *P* value of less than .05 was accepted as statistically significant.

RESULTS

The results of the SAXS analysis are as follows; small-angle data were recorded in the q range of 4-500 $Å^{-1}$, where q is the magnitude of the scattering vector. SAXS data for the 5 samples are presented in Fig. 1. The accuracy of the obtained structural sizes was in the range of 0.4-1.1 Å.

In the analysis of fractal dimension, as the negative slope (di) of the plots of LnI (q) and Lnq at regions where q is large provides information about the surface characteristics (LnI (q) – Lnq = di), the results indicated that the surface of the samples had small spherical formations. The fractal dimension (D_f) remained invariant in the range 1 < di < 3 across all samples after the fitting procedure (Table 1). As shown in Fig. 2, these values gave the information about the structural formation of the metallic samples.

Table 2 presents the effective radius of the particles (R_g) and the maximum distance between the nanoparticles (maximum extent) in Å, according to the analysis of distance distribution function. According to the minimum electron intensity and particle distance data, the lowest particle distance distribution was determined in Group II and then Groups IV, I, V and III were followed in order. The effect of annealing at argon atmosphere (Group IV) to the particle size and distance of the alloy was obvious than annealing at atmospheric condition (Group V).

Lamellar ordering may occur by slightly ordered cylindrical particles. Therefore, adoption of this model would appear to be appropriate for these types of surface morphologies. Table 3 presents the radius and length of the cylinders as well as the thickness of the layers for all groups

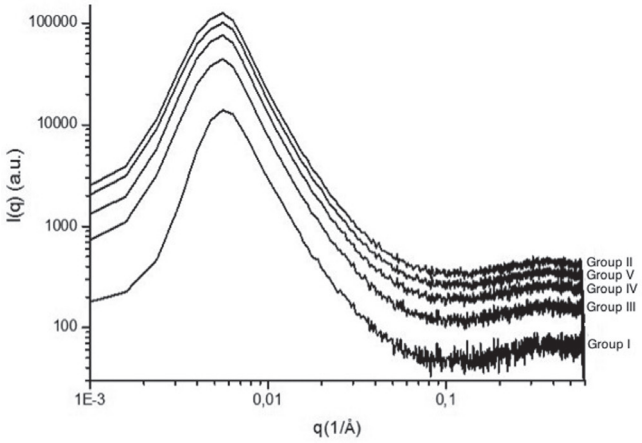

Fig. 1. SAXS patterns of the groups that were analyzed; q, magnitude of the scattering vector.

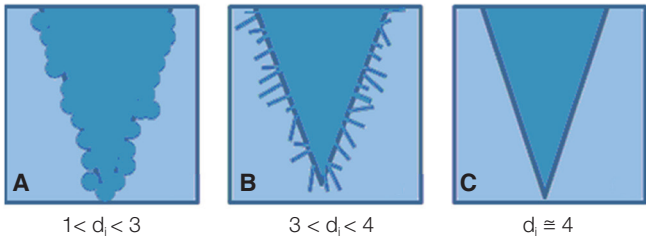

Fig. 2. Structure of materials shown schematically according to fractal dimension analysis. (A) mass fractals (1< d_i < 3, small spherical entities that have volumetric mass fractals with covered surfaces), (B) surface fractals (3 < d_i < 4, differently oriented and disjointed planks), (C) regular surfaces (d_i=4).

Table 1. Fractal dimension values

Group	D_f (fractal dimension)
I	2.76
II	2.74
III	2.48
IV	2.80
V	2.81

Table 2. Analysis results of distance distribution functions. Rg (Å), effective particule radius; maximum extent (Å), maximum distance between the nanoparticles

Group	Rg (Å)	maximum extent (Å)
I	303.94	820.17
II	272.43	717.76
III	306.05	829.56
IV	281.94	740.03
V	302.18	822.02

Table 3. Parameters obtained after the fitting procedure

Group	Scale	Radius (Å)	Length (Å)	Bilayer thickness (Å)
I	0.56	241.80	1418.27	16.87
II	0,39	232.39	2558.37	10.79
III	0.46	295.65	2588.02	14.24
IV	0.53	296.55	1598.50	7.11
V	0.47	278.22	1525.19	13.43

Table 4. Hardness conversion Table. Mean values of hardness of the specimens in Rockwell C, Brinell, Vickers and tensile strength

Group	Rockwell C hardness (HRC)	Brinell hardness (BHN)	Vickers hardness (HV)	Tensile strength (MPa)
I	47.39 ± 2.76	440	468	1545
II	42.86 ± 2.19	393	416	1350
III	48.16 ± 3.02	451	482	1586
IV	27.40 ± 3.98	268	277	900
V	34.42 ± 3.53	312	325	1093

of samples after the calculation of cylindrical and lamellar functions that were used for the fitting procedure. While Group IV presented the maximum radius of the cylinders, Groups III, V, I and II followed it by a decrease (Group IV > III > V > I > II). Likewise, Group III presented the maximum length of the cylinders and Groups II, IV, V, I followed it by a decrease (Group III > II > IV > V > I). Also, the bilayer thickness of the lamellas was decreased as follows: Group II > III > V > I > IV.

Mean Rockwell hardness (± SD) measurements, converted to Brinell and Vickers hardness values according to EN ISO 18265-App. G [27], and mean tensile strengths are presented in Table 4 for each group. The obtained hardness values of the groups aligned as follows in descending order: Group III > Group I > Group II > Group V > Group IV.

A statistically significant difference was observed between annealed groups (Groups IV and V) for hardness (P<.001) (Fig. 3).

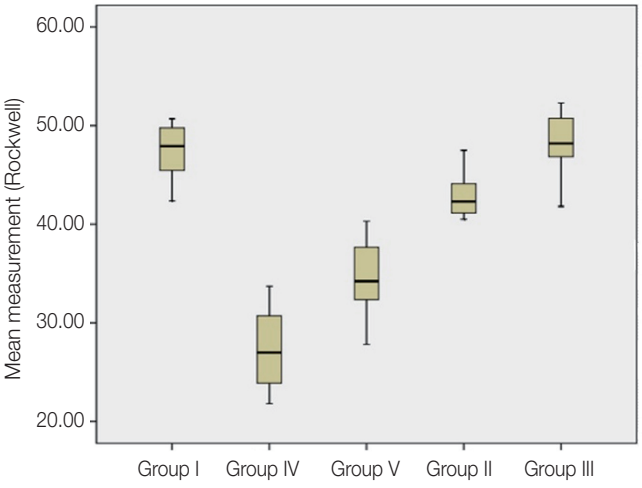

Fig. 3. Statistical results of the Rockwell measurements of the groups. Maximum hardness was measured in Group III (non-annealed) and minimum value was seen in Group IV (argon-annealed).

DISCUSSION

In dentistry, non-precious alloys are more widely used than precious alloys to manufacture metal sub-structures. Currently, the most commonly used non-precious alloys are nickel-chromium (Ni-Cr) and cobalt-chromium (Co-Cr) alloys.[2] However, the biocompatibility of Ni-Cr alloys has been questioned due to the possible damages to the health of patients and professionals in dental laboratories.[28,29] Wataha *et al.*[30,31] reported that the stability of Ni-Cr alloys was poor in acidic solutions or in the presence of acidic plaque, which causes the release of Ni. Thus, more biocompatible non-precious dental alloys would be preferable for metal ceramic restorations. Grimaudo[3] suggested that Co-Cr alloys were an alternative to Ni-Cr alloys in metal ceramic systems because they are more biocompatible, relatively well tolerated, and do not weaken the physical properties of metal-based porcelain restorations. Indeed, Co-based alloys are extensively used as wear- or corrosion-resistant

materials for metal sub-structures in fixed partial dentures.[32] Chromium (Cr), molybdenum (Mo), tungsten (W), nickel (Ni), and silicon (Si) are mainly used with Co-based dental alloys.[10,32] In particular, Cr is a strong carbide former and provides additional strength as a solute as well as resistance to corrosion and oxidation in the alloy.[32] In the present study, dental alloys based on Co-Cr were used to manufacture the samples for all groups.

In addition to the alloy structure, the manufacturing process influences the microstructure of the metal alloys. The wear resistance, mechanical properties, biocompatibility, and corrosion resistance may also be influenced by the microstructure, which depends on the thermal treatment applied to the material.[10] In dentistry, Co-Cr alloys with Mo or W can be manufactured by techniques such as casting, milling, and DMLS. In the present study, all of these manufacturing methods were used and compared in terms of the nanostructure and hardness of the resultant samples they produced.

Environmental factors affect the product quality in the casting and DMLS techniques. Bauer *et al.*[13] demonstrated that when noble and basic alloys are cast in an uncontrolled environment, the metals are exposed to deleterious gases and elements, which influence their mechanical properties such as internal porosity. DMLS is a new technology in dentistry for manufacturing Co-Cr metal ceramic substructures, and therefore, the steps of the procedure and the factors that affect product quality are not well known.

In the DMLS technique, Co-Cr nanoparticles fuse by applying Yb-fiber optic laser, and parts are built up layer by layer, each of which is 30 μm thick.[33] After completion of the manufacturing with DMLS, brittle and non-homogeneous metal objects are obtained.[10,11] For this reason, an annealing process must be applied for strength and homogeneity.[34] In the literature, annealing investigations have been performed on noble and semi-noble dental alloys.[24,35,36] Guo *et al.*[24] evaluated the effect of annealing on Pd-Ag dental alloys in a nitrogen atmosphere under different temperatures and reported that changes in temperature during annealing affect the microstructure and hardness of the alloy. In this study, the effects of annealing and different atmospheric conditions on Co-Cr dental alloys were tested to evaluate the changes in nanostructure and hardness.

The nanostructure was evaluated by SAXS analysis. The data from this analysis were also used in the analyses of the fractal dimensions, distance distribution function, and fitting function. Fractal dimension analysis gives information about surface characteristics. In the plot of LnI(q) – Lnq, the negative slope gives the value of "di" (Fig. 2). A di value of 4 signifies a nearly flat surface (very little irregularity of surface fractals); that of $3 < di < 4$ signifies surface fractals (differently oriented and disjointed planks); and that of $1 < di < 3$ signifies mass fractals (small spherical entities that have volumetric mass fractals with covered surfaces). According to the data of the present study, all groups were fit to the mass fractal structure ($1 < di < 3$) and exhibited a dendritic formation with small spherical entities irregularly stacked upon each other in layers. In literature, this dendritic arrangement is accepted as typical for Co-based dental alloys.[10,22] Interdendritic portions or carbide precipitation for Co-Cr alloys may be observed with different analysis techniques.[10]

Analysis of the distance distribution function provides information about the distances between particles, and the data of this analysis give the information about the homogeneity of the examining material. Comparison of the obtained data (Table II) showed that the effective radius of the particles (Rg) and the inter-particle distance (maximum extent) for Groups I, III, and V were similar to but greater than those for Groups II and IV. Nanostructural differences for the groups are attributed to the different manufacturing techniques. However, the difference between annealed groups (Groups IV and V) may be explained by the atmospheric conditions during annealing. The most homogeneous structure is expected in Group IV, as the manufacturing process accomplished completely.

Moreover, the data of the fitting function presented that all samples in the study displayed cylindrical rods and lamellas. The cylindrical function gives information about the structure of the cylinders of the samples. The radius and length of the cylinders also affect the length of the dendrites. According to the data of the cylindrical functions, Group I exhibited narrow and short cylinders. In Group II, these cylinders were much narrower and taller than those in Group I. Upon comparing the groups manufactured with DMLS, the following could be observed. In Group IV, the cylinders were nearly equal but much shorter than those in Group III; in Group V, the cylinders were narrower than those in Group III and shorter than those in Group IV. The lamellar function gives the information about the distance between the layers. Nomura *et al.*[37] and Telu *et al.*[38] also examined the lamellar formation of Co-Cr alloys by using XRD analysis. Telu *et al.*[38] showed that decreasing the bilayer thickness increased the homogeneity of the alloy. Across groups, the maximum and minimum bilayer thicknesses were observed in Groups I and IV, respectively. The results of the fitting function in the present study show that the most homogeneous group was Group IV. A detailed understanding of the precipitation process that occurs during annealing of these groups will require the use of a transmission electron microscope (TEM).

As mentioned before, the manufacturing conditions affect not only the structure but also the hardness of the alloys. Uncontrolled environments during casting and annealing adversely affect the mechanical properties of the alloy. The primary role of the furnace atmosphere in nonferrous annealing is to protect the product from excessive oxidation. To ensure this, the oxygen partial pressure of the atmosphere must be less than that necessary to form an oxide layer. In systems at atmospheric pressure, flushing with an inert gas (argon or nitrogen) is sufficient to reduce the oxygen level.[34] Mackert *et al.*[39] reported that when a Pd-Ag alloy was annealed in oxygen, hardness variations occurred owing to an increase in the oxidation layer. The

hardness comparisons in the present study showed that the argon atmosphere effectively reduced the hardness of Co-Cr alloys [Group IV < Group V]. The maximum hardness was observed in Group III. This suggests that the inner stresses after manufacturing, having caused increased brittleness of the alloy structure, also increased hardness. Under a noble gas atmosphere, the hardness decreases because of the decreased oxidation level. This acquired specification also increases the manipulability of the metal structure. A high quality product usually requires a bright finish, which is well known in an oral environment to reduce bacterial accumulation.[40] Thus, the use of an inert atmosphere should be critical for the appearance of the finished product. In a future study, observing the surface quality of metals manufactured with the DMLS technique and annealed in argon will be important. Furthermore, the structural changes and hardness values after porcelain firing cycles under different temperatures and porcelain-metal bonding characteristics of Co-Cr alloys should be investigated.

According to the analysis data and Rockwell hardness measurements, all groups behaved in different ways because of differences in manufacturing. The general nanostructure of the samples was composed of small spherical entities that were stacked atop one another in a dendritic form-a structure that may also be defined as cylindrically shaped clusters that includes spherical units. Although the effective radius of the spherical particles was very similar between the groups, the inter-particle distances differed. In addition, the radius and length of the cylinders as well as the thickness of the layers differed.

CONCLUSION

As the manufacturing with DMLS technique is becoming widespread in dentistry, the production steps should be well known. Especially, annealing is an important process in this technique. Increased inter-particle distance and increased bilayer thickness for non-annealed alloys indicate a non-homogeneous form and long dendrites. For the decreased hardness and homogeneity of the Co-Cr metal ceramic substructures annealing in argon atmosphere is essential. Annealing in oxygen relieves the inner stresses but the layers could not get closer and thus the hardness increase. For this reason, it must be well known by the prosthodontist that annealing environment is also important for DMLS manufacturing of the Co-Cr dental alloys.

REFERENCES

1. Wataha JC. Biocompatibility of dental casting alloys: a review. J Prosthet Dent 2000;83:223-34.
2. Pretti M, Hilgert E, Bottino MA, Avelar RP. Evaluation of the shear bond strength of the union between two CoCr-alloys and a dental ceramic. J Appl Oral Sci 2004;12:280-4.
3. Grimaudo NJ. Biocompatibility of nickel and cobalt dental alloys. Gen Dent 2001;49:498-503.
4. Dobrzański LA, Reimann L. Influence of Cr and Co on hardness and corrosion resistance CoCrMo alloys used on dentures. J Achieve Mater Manuf Eng 2011;49:193-9.
5. Karpuschewski B, Pieper HJ, Krause M, Döring J. In: Schuh G, Neugebauer R, Uhlmann E, eds. Future trends in production engineering (Proceedings of the first conference of the German Academic Society for production engineering. Berlin, Germany, 8th-9th June 2011, 1st ed. Springer, New York; 2013.
6. Fasbinder D. Using digital technology to enhance restorative dentistry. Compend Contin Educ Dent 2012;33:666-8.
7. Miyazaki T, Hotta Y, Kunii J, Kuriyama S, Tamaki Y. A review of dental CAD/CAM: current status and future perspectives from 20 years of experience. Dent Mater J 2009;28: 44-56.
8. Aboushelib MN, Elmahy WA, Ghazy MH. Internal adaptation, marginal accuracy and microleakage of a pressable versus a machinable ceramic laminate veneers. J Dent 2012;40: 670-7.
9. Figliuzzi M, Mangano F, Mangano C. A novel root analogue dental implant using CT scan and CAD/CAM: selective laser melting technology. Int J Oral Maxillofac Surg 2012;41:858-62.
10. Jevremovic D, Puskar T, Kosec B, Vukelic D, Budak I, Aleksandrovic S, Egbeer D, Williams R. The analysis of the mechanical properties of F75 Co-Cr alloy for use in selective laser melting (SLM) manufacturing of removable partial dentures (RPD). Metal 2012;51:171-4.
11. Hollander DA, von Walter M, Wirtz T, Sellei R, Schmidt-Rohlfing B, Paar O, Erli HJ. Structural, mechanical and in vitro characterization of individually structured Ti-6Al-4V produced by direct laser forming. Biomaterials 2006;27:955-63.
12. Rodrigues WC, Broilo LR, Schaeffer L, Knörnschild G, Espinoza FRM. Powder metallurgical processing of Co-28%Cr-6%Mo for dental implants: Physical, mechanical and electrochemical properties. Powder Tech 2011;206:233-8.
13. Bauer JR, Grande RH, Rodrigues-Filho LE, Pinto MM, Loguercio AD. Does the casting mode influence microstructure, fracture and properties of different metal ceramic alloys? Braz Oral Res 2012;26:190-6.
14. Gill P, Munroe N, Pulletikurthi C, Pandya S, Haider W. Effect of Manufacturing Process on the Biocompatibility and Mechanical Properties of Ti-30Ta Alloy. J Mater Eng Perform 2011;20:819-823.
15. Manfredi D, Calignano F, Krishnan M, Canali R, Ambrosio EP, Atzeni E. From powders to dense metal parts: Characterization of a commercial AlSiMg alloy processed through direct metal laser sintering. Materials 2013;6:856-69.
16. Tandon R. In: Disegi JA, Kennedy RL, Pilliar R, eds. Cobalt Base Alloys for Biomedical Applications ASTM STP 1365. American Society for Testing and Materials, West Conshohocken, PA, 1999.
17. Bolzoni L, Esteban PG, Ruiz-Navas EM, Gordo E. Mechanical behaviour of pressed and sintered titanium alloys obtained from master alloy addition powders. J Mech Behav Biomed Mater 2012;15:33-45.
18. Lohfeld S, McHugh PE. Laser sintering for the fabrication of

tissue engineering scaffolds. Methods Mol Biol 2012;868:303-10.
19. Castillo-de-Oyagüe R, Sánchez-Turrión A, López-Lozano JF, Albaladejo A, Torres-Lagares D, Montero J, Suárez-García MJ. Vertical misfit of laser-sintered and vacuum-cast implant-supported crowncopings luted with definitive and temporary luting agents. Med Oral Patol Oral Cir Bucal 2012;17:e610-7.
20. Traini T, Mangano C, Sammons RL, Mangano F, Macchi A, Piattelli A. Direct laser metal sintering as a new approach to fabrication of an isoelastic functionally graded material for manufacture of porous titanium dental implants. Dent Mater 2008;24:1525-33.
21. Girardin E, Renghini C, Dyson J, Calbucci V, Moroncini F, Albertini G. Characterization of porosity in a laser sintered MMCp using X-ray synchrotron phase contrast microtomography. Mater Sci Appl 2011;2:1322-30.
22. Gaytan SM, Murr LE, Martinez E, Martinez JL, Machado BI, Ramirez DA, Medina F, Collins S, Wicker RB. Comparison of Microstructures and mechanical properties for solid and mesh cobalt-base alloy prototypes fabricated by electron beam melting. Metall Mater Trans A 2010;41:3216-27.
23. Chen CL, Tatlock GJ, Jones AR. Effect of annealing temperatures on the secondary re-crystallization of extruded PM2000 steel bar. J Microsc 2009;233:474-81.
24. Guo WH, Brantley WA, Li D, Clark WA, Monaghan P, Heshmati RH. Annealing study of palladium-silver dental alloys: Vickers hardness measurements and SEM microstructural observations. J Mater Sci Mater Med 2007;18:111-8.
25. Porod G. In: Glatter O, Kratky O, eds. Small angel X-ray scattering. Academic Press Inc, London, UK, 1982.
26. Martin JE, Hurd AJ. Scattering from fractals. J Appl Crystallogr 1987;20:61-78.
27. EN ISO 18265: 2005, Metallic materials - Conversion of hardness values.
28. Bezzon OL, Ribeiro RF, Rollo JM, Crosara S. Castability and resistance of ceramometal bonding in Ni-Cr and Ni-Cr-Be alloys. J Prosthet Dent 2001;85:299-304.
29. Kern M, Thompson VP. Durability of resin bonds to a cobalt-chromium alloy. J Dent 1995;23:47-54.
30. Wataha JC, Lockwood PE. Release of elements from dental casting alloys into cell-culture medium over 10 months. Dent Mater 1998;14:158-63.
31. Wataha JC, Nelson SK, Lockwood PE. Elemental release from dental casting alloys into biological media with and without protein. Dent Mater 2001;17:409-14.
32. Liu R, Xi SQ, Kapoor S, Wu XJ. Effects of chemical composition on solidification, microstructure and hardness of Co-Cr-W-Ni and Co-Cr-Mo-Ni alloy systems. Int J Res Rev Appl Sci 2010;5:110-22.
33. Iseri U, Ozkurt Z, Kazazoglu E. Shear bond strengths of veneering porcelain to cast, machined and laser-sintered titanium. Dent Mater J 2011;30:274-80.
34. ASM Handbook Vol. 4, Heat Treating. ASM International, Ohio, 1991.
35. Tani T, Udoh K, Yasuda K, Van Tendeloo G, Van Landuyt J. Age-hardening mechanisms in a commercial dental gold alloy containing platinum and palladium. J Dent Res 1991;70:1350-7.
36. Kim HI, Lee DH, Sim JS, Kwon YH, Seol HJ. Age-hardening by miscibility limit of Au-Pt and Ag-Cu systems in an Au-Ag-Cu-Pt alloy. Mater Character 2009;60:357-62.
37. Nomura N, Abe M, Kawamura A, Fujinuma S, Chiba A, Masahashi N, Hanada S. Fabrication and mechanical properties of porous Co-Cr-Mo alloy compacts without Ni addition. Mater Trans 2006;47:283-6.
38. Telu S, Patra A, Sankaranarayana M, Mitra R, Pabi SK. Microstructure and cyclic oxidation behavior of W–Cr alloys prepared by sintering of mechanically alloyed nanocrystalline powders. Int J Refract Met Hard Mater 2013;36:191-203.
39. Mackert JR Jr, Ringle RD, Fairhurst CW. High-temperature behavior of a Pd-Ag alloy for porcelain. J Dent Res 1983;62:1229-35.
40. McGinley EL, Coleman DC, Moran GP, Fleming GJ. Effects of surface finishing conditions on the biocompatibility of a nickel-chromium dental casting alloy. Dent Mater 2011;27:637-50.